Biogeosciences Discuss., 4, 1405–1435, 2007
www.biogeosciences-discuss.net/4/1405/2007/

Biogeosciences Discussions

Biogeosciences Discussions is the access reviewed discussion forum of *Biogeosciences*

Characterizing ecosystem-atmosphere interactions from short to interannual time scales

M. D. Mahecha[1], M. Reichstein[1], H. Lange[2], N. Carvalhais[3], C. Bernhofer[4], T. Grünwald[4], D. Papale[5], and G. Seufert[6]

[1]Max-Planck-Institute for Biogeochemistry, Jena, Germany
[2]Norwegian Forest and Landscape Institute, Ås, Norway
[3]Environmental System Analysis Group, New University of Lisbon, Portugal
[4]Deptartment of Meteorology, Technical University of Dresden, Germany
[5]Department of Forest Science and Environment, University of Tuscia, Viterbo, Italy
[6]Climate Change Unit, European Comission – Joint Research Centre, Ispra, Italy

Received: 3 April 2007 – Accepted: 23 April 2007 – Published: 2 May 2007

Correspondence to: M. D. Mahecha (miguel.mahecha@bgc-jena.mpg.de)

Abstract

Characterizing ecosystem-atmosphere interactions in terms of carbon and water exchange on different time scales is considered a major challenge in terrestrial biogeochemical cycle research. The respective time series are now partly comprising an observation period of one decade. In this study, we explored whether the observation period is already sufficient to detect cross relationships of the variables beyond the annual cycle as they are expected from comparable studies in climatology.

We explored the potential of Singular System Analysis (SSA) to extract arbitrary kinds of oscillatory patterns. The method is completely data adaptive and performs an effective signal to noise separation.

We found that most observations (NEE, GPP, R_{eco}, VPD, LE, H, u, P) were influenced significantly by low frequency components (interannual variability). Furthermore we extracted a set of nonlinear relationships and found clear annual hysteresis effects except for the NEE-R_g relationship which turned out to be the sole linear relationship in the observation space. SSA provides a new tool to investigate these phenomena explicitly on different time scales. Furthermore, we showed that SSA has great potential for eddy covariance data processing since it can be applied as novel gap filling approach relying on the temporal time series structure only.

1 Introduction

Measurements from eddy covariance towers provide time series of CO_2, H_2O, and energy fluxes permitting to characterize the temporal development of ecosystem-atmosphere interactions (Aubinet et al., 2000; Baldocchi, 2003). The data are globally collected within a variety of international projects (e.g., CarboEuropeIP, Fluxnet-Canada, Ameriflux). Currently, many sites are close to complete the first decade of continuous flux records, permitting ecosystem fluxes to be investigated on a variety of time scales beyond seasonal and annual cycles (Baldocchi, 2003; Saigusa et al., 2005;

Wilson and Baldocchi, 2000). The observed fluxes can be regarded as ecophysiological responses to meteorological and climatological conditions but also to any other type of external and intrinsic ecosystem modifications (Baldocchi, 2003), and thus, the observed flux variability can be attributed at least partly to the variability of the driving variables (Law et al., 2002).

The time scale dependencies of cross relationships between the variables are quite well understood on the short term (from hours to seasonal patterns) in a variety of micro-meteorological, ecophysiological and statistical aspects. Moreover it is well known that some of the driving variables (e.g., temperature and precipitation) depict climate induced low frequency oscillations and trends (Ghil and Vautard, 1991; Plaut and Vautard, 1994; Paluš and Novotná, 2006). A self-evident hypothesis is whether long term temporal structures are detectable in existing flux data, given the current time series length. Consequently, much effort has been done since the initial eddy covariance measurement setups to investigate ecosystem flux variability beyond the annual cycle (e.g., Goulden et al., 1996), which is crucial for assessing ecosystems under changing environmental conditions (Dunn et al., 2007). In this context, three main questions arise: (a) can we identify and provide accurate descriptions of flux variability on different temporal scales? (b) Is it possible to detect and describe the statistical properties of "interannual variability"; (c) are (possibly nonlinear) trends identifiable in the time series? All of these are tied to the problem of identifying and separating the relevant time scales of the observed time series.

Related research fields have already provided a variety of approaches for the investigation of time series on multiple time scales including low frequency oscillations and trends (von Storch and Zwiers, 1999). One successfully applied method for extracting signals from time series is "Singular System Analysis" (SSA), an approach originating in systems dynamics (Broomhead and King, 1986) and successfully applied to hydrometeorology (Shun and Duffy, 1999), climatology (Plaut and Vautard, 1995; Ghil et al., 2002; von Storch and Zwiers, 1999), and hydrology (Lange and Bernhardt, 2004). This study aims at exploring the potential of SSA in the context of eddy covariance flux data.

The method is highly superior to the well known Fourier analysis, since it is fully phase and amplitude modulated (Allen and Smith, 1996). The idea is that each observed time series is a set of (linearly) superimposed subsignals (Golyandina et al., 2001). In other words, we investigated whether SSA could provide an option to extract components of ecosystem fluxes corresponding to different time scales. Partitioning a time series into subsignals is thought to separate long term signals from the annual cycle and high frequency components. All the same, this study addresses some special properties of the eddy covariance data. This is of concern for example for the typical occurrence of very large gaps due to power outage, where the already tested gap filling tools do not provide satisfactory results since they rely on the meteorological variables. For this, a recent SSA extension could be helpful which is able to fill missing values based on the temporal correlation structure of the time series (Kondrashov and Ghil, 2006).

Our goal in this study was to give a short methodological introduction to SSA, including test statistics, and the derived gap filling strategy. The results and discussion focuses on the variance allocation of different time scales in a set of fundamental observations. These are net ecosystem exchange *NEE*, gross primary productivity *GPP*, ecosystem respiration R_{eco}, temperature *T*, global radiation R_g, precipitation *P*, vapor pressure deficit *VPD*, latent heat *LE*, sensible heat *H*, and wind speed *u*. Their temporal behaviour and cross relationships are explored on different time scales. Finally, the methodological chances and limitation for future data adaptive ecosystem assessments and forecasts are highlighted.

2 Method

2.1 Singular System Analysis

The goal of SSA is to identify subsignals of a given time series $X(t)$ and to project them to the corresponding scales. The time series (centered to zero mean) is subjected to SSA, which can be described as a two step procedure consisting of a signal decomposition and a signal reconstruction (Golyandina et al., 2001). The decomposi-

tion aims at finding relevant orthogonal functions which allows to reconstruct the time series partially or, if required, entirely.

The analysis first needs the a priori definition of an embedding dimension which is a window of length P. Sliding the window along the time series leads to a trajectory matrix, consisting of the sequence of $K=N-P+1$ time lagged vectors of the original series. The P dimensional vectors of the trajectory matrix $\mathbf{Z}$ are set up as described in Eq. (1), (Golyandina et al., 2001).

$$Z_i = (X(i), \ldots, X(i+P-1))^T, 1 \le i \le K \tag{1}$$

Based on the trajectory matrix $\mathbf{Z}$ a $P \times P$ covariance matrix $\mathbf{C}=\{c_{i,j}\}$ is built which according to Vautard and Ghil (1989) can be estimated directly from the data in form of a Toeplitz matrix; see Eq. (2).

$$c_{i,j} = \frac{1}{N-\mid i-j \mid} \sum_{t=1}^{N-|i-j|} X(t)X(t+\mid i-j \mid) \tag{2}$$

The entries of the matrix depend on the lag $\mid i-j \mid$ only, and thus, the captured covariance is dependent on the embedding dimension P. Based on the lag-covariance matrix one is able to find the orthonormal basis by solving Eq. (3).

$$\mathbf{E}^T\mathbf{C}\mathbf{E} = \mathbf{\Lambda} \tag{3}$$

In this equation $\mathbf{E}$ is a $P \times P$ matrix containing the eigenvectors E_j, also called empirical orthogonal functions (EOF's) of $\mathbf{C}$. The matrix $\mathbf{\Lambda}$ contains the respective eigenvalues in the diagonal, sorted by convention in descending order $diag(\mathbf{\Lambda})=\lambda_1, \ldots, \lambda_P$. It can be shown that due to the properties of covariance matrix $\mathbf{C}$, preserving symmetry, being real valued and positive semidefinite, all eigenvectors and eigenvalues are itself real valued, where the latter are nonnegative scalars. The eigenvalues are proportional to the fraction of explained variance corresponding to each EOF. In analogy to the well known Principal Component Analysis (PCA) the decomposition allows the construction

of principal components as generated time series representing the extracted orthogonal modes (Eq. 4). This is why SSA is often also called a "PCA in the time domain".

$$A^\kappa(t) = \sum_{j=1}^{P} X(t+j-1)E^\kappa(j) \tag{4}$$

The κth principal components of the time series can be regarded itself as a time series of length K. A typical phenomenon is the appearance of two principal components of almost identical structure and period length but with opposite parity (phase shift $\pi/2$). This can be explained by the fact that the representation of periodic modes requires at least two linear PCs (Hsieh and Wu, 2001).

The last step in SSA is the reconstruction of the time series through the principal components $A^\kappa(t)$, see Eq. (5). The original signal can be fully or just partially reconstructed. At this selective step the analyst has to decide which $A^\kappa(t)$ are combined so that one obtains an interpretable combination of principal components. This step enables signal-noise separation and the reconstruction of specifically selected frequency components, as illustrated by Eq. (5).

$$R^k(t) = \frac{1}{M_t} \sum_{\kappa \in k} \sum_{j=L_t}^{U_t} A^\kappa(t-j+1)E^\kappa(j) \tag{5}$$

In this reconstruction procedure, k is an index set, M_t is a normalization factor and corrections for the series boundaries are given by L_t and U_t (see definitions in 2.1).

$$(M_t, L_t, U_t) = \tag{6}$$

$$\begin{cases} \left(\frac{1}{t}, 1, t\right) & \text{for } 1 \le t \le P-1, \\ \left(\frac{1}{P}, 1, P\right) & \text{for } P \le t \le K, \\ \left(\frac{1}{T-t+1}, t-T+P, P\right) & \text{for } K+1 \le t \le T. \end{cases}$$

2.1.1 Signal selection and separability

The selective time series reconstruction opens the chance to depict the behavior of the series explicitly on different temporal scales. Obviously, the finest resolution can be found reconstructing the series individually for each mode, or for each pair of oscillatory modes. Whether two components set up an oscillatory pair has to be checked manually for modes of similar dominant frequency. Golyandina et al. (2001) described this heuristic procedure as "Caterpillar SSA" which is also beneficial for detecting unexpected oscillations. This is facilitated by reordering the eigenvalues according to the dominant frequency of the belonging EOF (Allen and Smith, 1996). After normalizing the eigenvalues this illustrates the variance allocation on the identified dominant frequencies. This picture can be seen as a "discretized power spectrum" (Shun and Duffy, 1999) which is commonly called the "eigenspectrum" of a given series.

However, the eigenspectrum does not surmount the critical point to find a heuristic approach of signal selection for the subsequent interpretations. An useful alternative is to test the null hypothesis that the SSA output is compatible with a red noise assumption. The assumption of "red noise" seems the most appropriate null hypothesis in geosciences since many records (e.g., air and sea surface temperature, river runoff, climate indices) usually depict "reddened" spectral properties (Ghil et al., 2002). In fact, this can also be shown for *NEE* time series from the eddy covariance measurements by investigating their specific autocorrelation which is non trivial. This can be seen as a statistical validation for the "red noise" null hypothesis (Richardson et al., 2007[1]).

Several Monte Carlo SSA (MCSSA) approaches were developed for testing whether the eigenspectrum is compatible with an equivalent spectrum corresponding to a set of surrogate data generated through an autoregressive process of first order ($AR(1)$; for different test variants see, e.g., Allen and Smith, 1996; Paluš and Novotná, 1998). Here, we followed a computational much more effective straight forward approach,

[1]Richardson, A. D., Mahecha, M. D., Falge, E., et al.: Statistical properties of random CO_2 flux measurement uncertainty inferred from model residuals, under review, 2007.

introduced by Shun and Duffy (1999), where the analytic expression for the red noise spectrum is fitted to the eigenspectrum:

$$\phi(f) = \frac{a}{[b + (2\pi f)^2]} \tag{7}$$

In this equation, a and b are process parameters, whereas f represents the observed frequencies. The model is first fitted to the overall eigenspectrum and a 95% confidence interval is calculated. The fit is then repeated for the nonsignificant fraction of the eigenspectrum only. This repetitive model fitting is stopped if no additional significant modes are identified. This approach is not very common, thus, we run several tests for the present study where the standard MCSSA proposed by Allen and Smith (1996) based on more than 300 iterations showed to produce similar results than the above model given by Shun and Duffy (1999).

2.2 SSA for time series with missing values

A fundamental problem for the eddy covariance towers is the intricate measurement setup leading to gaps of varying length, from hours to months (Katul et al., 2001). The primary gap filling on half-hourly data is possible through a variety of methods which do not lead to fundamental differences (for a broad comparison see Moffat et al., 2007[2]). However, the available gap-filling methods fail in the presence of large gaps, where no secondary information, e.g., on meteorological conditions is available. Here, a different strategy has to be adopted where the gaps have to be filled based on the temporal correlation structure of the time series itself. Katul et al. (2001) showed that such situations do not necessarily limit the investigation of eddy covariance data in the frequency domain and can be assessed by means of wavelet analysis. They state to be able to "remove the effect of missing values on spectral and co-spectral calculations". All the same, this did not provide a tool for filling the large time series gaps.

[2]Moffat, A., Papale, D., Reichstein, M., et al.: Gap filling methods intercomparison, under review, 2007.

Kondrashov and Ghil (2006) introduced an iterative SSA gap filling strategy, which allows (in the above introduced sense) a time series reconstruction for fragmented time series. This provides both, a chance for applying SSA to fragmented records and an explicit tool for gap filling. The method consists of a two-loop gap filling which for the sake of simplicity is described here in form of a "how to" recipe:

1. The first step is to remove the time series mean, where the mean is estimated from the present data only.
2. A inner loop iteration starts as SSA of the zero padded time series. The leading (highest eigenvalue) reconstructed component (RC) is used to fill the values in the gaps. This allows a new estimate on the time series mean, which is used for a new centering where the padded values are set to their reconstructions. This procedure is carried out, based on the computed and recomputed RC's until a convergence criterion is met. Since the original publications did not specify the type and value of convergence, we used the correlation coefficient between the subsequently filled time series, and stopped the iteration when r^2>0.98.
3. After the first inner loop iteration meets the convergence criterion, the method switches to an outer loop iteration. This is the natural extension of the above described procedure, by simply adding a second (third etc.) new reconstructed component to inner loop iteration.

2.3 Eddy covariance data processing

The eddy covariance data were collected based on a 20 Hz sampling frequency and subsequently aggregated to an half hourly integration interval (Aubinet et al., 2000). The CO_2 data were corrected for canopy storage and u_* filtered to avoid measurements of insufficient turbulence (Papale et al., 2006).

The obvious approach is to use SSA for gap-filling these data and carrying out the subsequent analysis based on the half hourly data was discarded due to the computational limitation of SSA. Furthermore this study aims at inferring explicitly the low

frequency modes in the time series. In general the SSA bottleneck constructing the lag-covariance matrix limits the application to time series with several thousands of observations. Hence, we followed a double gap filling strategy. We used the method provided by Reichstein et al. (2005, Appendix A), which is a locally data adaptive look up table to fill missing values on half hourly basis. The subsequently aggregated data receive quality flags indicating the amount of filled data per day. An aggregated daily value is considered as missing if the amount of original observations falls below 0.9. Only these values were filled by the SSA gap filling strategy.

2.4 Site description

The eddy covariance data were measured at the Station "Tharandt" (50°57′49″ N, 13°34′01″, 380 m a.s.l.) which is ca. 25 km SW from Dresden, Germany, corresponding to a suboceanic/subcontinental climate. Long term meteorological records indicate a mean annual air temperature of 7.8°C, and a mean annual precipitation sum of 823 mm. The dominant wind direction is SW. The area was episodically affected by summer droughts. "Tharandt" is a spruced stand (72% *Picea abies* L. (Karst.)) since 1987, mixed with further coniferous evergreen (15%) and descideous species (13%). A detailed description of the environmental conditions of the site, including descriptions of the EC data recording and meteorological data is given by Grünwald and Bernhofer (2007).

3 Results and discussion

3.1 Significant frequencies and variance allocation

The eigenspectra for the analysed ecosystem variables (*NEE*, *GPP*, R_{eco}, *VPD*, *P*, *T*, R_g, *LE*, *H* and *u*; Fig. 1) reveal a set of nontrivial patterns; a whole gamut of significant frequencies modes was found in the time series. The identified components are quantitatively summarized in Table 1, where all results are based on an embedding dimension of $\frac{N}{P}$=2.5.

Analysing the eigenspectra from the low to the high frequency domain shows that several variables are significantly driven by interannual variability (Table 1). The derived carbon and energy fluxes, *GPP*, R_{eco}, *LE*, and *H* depict significant modes at the very edge of their eigenspectra indicating the presence of even longer term structures than effectively describable by the applied embedding procedure. These non extractable subsignals from minimum frequency EOF's can be either oscillations or trends, which is not decidable at the given time series length. In the following, these patterns will be summarized as edge cycles. It is important to note that similar components are also contained in most of the other variables but not on a significant level so that in the overall view we expect that the signals contain more low frequency modes.

Apart from the identified edge cycles, most time series depict oscillations with periods around 1.4, 1.7, 1.8 and 2.3 yr, except *T*. The question remains why *T* does not depict low frequencies modes within the observation period when even R_{eco} which is estimated from *NEE*, *T* and a reference respiratory component does so. It is a well known phenomenon in the northern hemisphere that temperature depicts a set of oscillatory patterns and trends beyond the annual scale, (e.g., Ghil and Vautard, 1991). For example quasi biennial oscillations in the climate system can be nicely seen in temperature records and also traced back to the NAO index (Paluš and Novotná, 2006). The absence of similar observations could be an artifact of the very short record.

Regarding the annual cycle it is obvious that it explains most of the variance in all fluxes, except for precipitation *P* which exhibits a very peculiar behavior in the overall eigenspectrum. The *P*-eigenspectrum indicates that one can assume that we are dealing with an almost entirely noise dominated signal (97.2% of the signal is compatible with the red noise model) which is consistent with previous findings in literature (Shun and Duffy, 1999; Tessier et al., 1996) if the temporal resolution is not too small (e.g. daily). On very small time scales, however, also rainfall exhibits a rather intriguing multiscaling behavior (Peters et al., 2002).

Furthermore SSA extracted many high frequencies components. Noticeable a semiannual component was found to be common to most ecosystem variables where the

exceptions are again *T* and *P*. In the overall view one has to take into account the relative importance of the different subsignals, where for some variables (e.g., *GPP*, *H*, *LE*, and *u*) the high frequency components are essential in terms of allocated variance.

The results of the eigenspectra rely on the decomposition of time series lag covariance structure as described in Eq. (3). Yet, only the subsequent time series reconstruction gives insights into the effective behaviour of the observation on the respective time scale. Figure 2 gives an example for the reconstruction of *NEE*. The figure shows also clearly that it is not decidable whether the interannual variability is a sinusoidal oscillation or a true trend. Furthermore, the semiannual component depicts a strong amplitude modulation indicating that its importance in the time series structure is also time dependent. It can also seen how a substantial part of the time series variance (38.1%) can be attributed to what was declared "red noise" by the test set up. Finally, the bottom panel is an example how the fundamental time evolution of *NEE* was reconstructed, based on very few significant noise free modes.

3.2 Scale dependent *NEE*-*T* relationships

As highlighted in Table 1 and Fig. 1 it was possible to reveal that the different variables are dominated by a variety of subsignals which can be partly attributed to comparable frequency classes. Thus, it is possible to assess the cross relationships of the data explicitly on the identified time scale, rather than establishing empirical relationships from the entire observation space as it is the standard approach in most classical regression approaches.

Figure 3 shows the relationship between *NEE* and *T* where different components are plotted versus each other. The relationship between the pure annual components of both variables depicts a clear hysteresis effect (Fig. 3, left panel). Furthermore one sees that the red noise component is apparently not containing major information on the cross relationships of the two. If the significant interannual component is added to the annual cycles, the mentioned hysteresis effect is modified (Fig. 3, centre panel). Although the interannual component accounts only for a small part of the data variability (Table 1), the figure shows clearly that this is sufficient to induce a trend in the summer

fluxes toward decreased carbon uptake. By contrast the observed loss of carbon during the winter days found by the relationship of the annual components is neutralized by the inter annual component. The problem is that these components are not the only significant part of the time series and the intraannual component also plays a crucial role in the flux data and their contribution induces a feasible and complex variability (Fig. 3, right panel). The overall picture of the *NEE-T* relationship is nonlinear and it is obvious that dealing with cross relationships of flux data is a temporal multilayer problem.

It has been mentioned above that the interannual variability is neither contributing much to overall time series variability, nor allocates great amounts of carbon. In spite of that we have to state now that the contribution of the interannual variability could be essential for assessing the ecosystem under climate change conditions, given the observed forcing of this component, to the entire flux observations. Moreover models have difficulties to explain interannual variability. Our findings corroborate the assumption that interannual variability is a major qualitative contribution required to describe the temporal behaviour of the net carbon balance in terrestrial ecosystems.

3.3 Nonlinear ecosystem-atmosphere interactions

There was evidence that similar nonlinear patterns as found in the *NEE-T* space are influencing the relationships between *NEE* and *GPP*, *VPD*, *u*, *LE*, or *H* as well. Figure 4 shows how these variables are linked when inferred from a joint reconstruction of their annual and interannual components. The ecosystem behaviour on this temporal scale is highly nonlinear, and we observe several hysteretic effects. These hysteresis loops are particularly well pronounced in terms of *NEE-VPD*, *NEE-u*, and *NEE-H* dependencies. Less clear patters were found in the *NEE-LE* space and the carbon cycle relationship *NEE-GPP*.

Above all, it turned out that the sole linear dependency on annual time scales can be found when relating *NEE* to R_g. Having seen that cross relationships of RC's originating from different variables can exhibit a wide range of nonlinearities, this occurrence of a linear relation is by no means trivial. Whether this phenomenon is unique for the in-

vestigated site and related to the dominance of evergreen coniferous species (implying low variations of the leaf area index) or a more general phenomenon requires further investigations. However, this observation is in accordance with previous findings which showed that R_g provides a good basis for modelling terrestrial carbon fluxes.

In the overall view most cross relationships between the ecosystem variables contain more or less pronounced hysteresis effects (Fig. 4). Especially for the case of *T* exists a sound explanation: Owing to a R_g-*T* hysteresis the shown nonlinear *NEE-T* dependence is an imparted effect. From an ecological point of view this might appear trivial and can be understood as the time varying ecosystem heat capacity in the curse of the seasonal cycle. Indeed, the existence of hysteretic behaviour of ecosystem-atmosphere interactions is well known (e.g., the *T-NEE* relationship on short time scales; Nakai et al., 2003). However, here we present new evidence on the occurrence of a well pronounced hysteresis on annual scales which was not yet reported in the literature. As far as the magnitude of impact is concerned, this is of fundamental importance for further tasks of ecosystem modelling. Apart of the "obvious" *T-NEE* example, the causes for the unexpected but equally well pronounced hysteresis effects, e.g. in the *NEE-u* or *NEE-VPD* relationships, remain unclear. This could lead to further questions, for example what does the existence of an annual cycle in wind velocity mean for the turbulent exchange of CO_2, H_2O, and energy? Furthermore, we presume that these observations of hysteresis lead to more general problems in ecosystem theory, for example whether additional investigations of hysteretic ecosystem-atmosphere exchanges could contribute to a better understanding of ecosystem memory. This is of relevance for the quantification of lag effects in ecosystem responses to any type of reoccurring phenomena on a variety of time scales, including summer droughts or winter anomalies. An example is given here by the *NEE-H* relationship (Fig. 4, lower central panel), where a clear deviation of the hysteretic behaviour happens precisely during the summer heat wave in 2003 (cf. Ciais et al., 2005; Granier et al., 2007; Reichstein et al., 2007, for a comprehensive discussion of this climate anomaly).

Asides from the clear nonlinear relationships of the described annual-interannual

RC's, Fig. 4 shows also the red noise components for these variables. As it was shown in Fig. 1, the red noise fraction comprises most of the high frequency components of the time series. When contrasting these components with the annual-interannual components we came across that there might be different types of relationships acting on different time scales. This phenomenon is highlighted for example when confronting the red noise fraction in the *NEE-GPP* space with their respective annual-interannual RC's (Fig. 4, upper left pannel). In this particular case, simple linear regression analysis would lead to systematically varying parameters depending on the time scale of concern. Interestingly, the red noise *NEE*-R_g relationship depicts a slightly nonlinear relationship which is an intuitive example how the analysis of the entire signal could obscure the inherent linearity of their cross relationship on an annual scale.

3.4 Methodological observations, limitations and outlook

The results presented here show both, the strength and pitfall of SSA. The clear advantage is that the method is entirely data driven, thus the extracted patterns as provided by the explicit reconstructions on the different time scales can be seen as "empirical flux-variance partitioning". Of course, fundamental patterns as the annual cycle can be identified also by a linear combination of weighted sines and cosines as it is commonly applied in terms of Fourier analysis. This could lead to similar results in fully homogeneous subsignals, which is however not expected to be the case in real world data. For phase and amplitude varying signals, e.g., as it was shown here very clearly for the seminannual cycle of *NEE*, two EOF's are fully sufficient whereas a Fourier type analysis would require a highly parameterized "model".

The critical point in SSA is the choice of the embedding dimension P, which is a compromise between two goals: The first is to maximize the information content of the analysis requiring a large window length P. The second is to optimize the statistical confidence of the decomposition, achieved through a high number of channels K. A different strategy could be to optimize the embedding dimension such that the extracted signals are well separable avoiding a signal superimposition in the RC's (Golyandina et al., 2001). Empirical findings in literature suggest to range the embedding dimension

from $\frac{N}{P}$=11 (Ghil et al., 2002) to $\frac{N}{P}$=2.5 (Lange and Bernhardt, 2004). Owing to the objective of this study to explore explicitly long range structures in the data, we used the lowest value reported in literature $\frac{T}{P}$=2.5. The quality of signal separability obtained by a further decrease of this ratio turned out to be unfeasible since most extracted RC's could be seen as a new set of superimposed signals (for an accurate definition of signal separability cf. Golyandina et al., 2001). However, increasing the ratio did not lead to a better signal separability and was not justified here. Due to the short observation period of eight years only, we had to use a maximum window length to be able to find long range structures. We found that the identified frequencies and their respective variance allocations remains fairly stable over a certain range of embedding dimensions. Major shifts in the variance allocations in the frequency domain occur mainly in the low frequency modes (f<1yr^{-1}) due to the decrease of correlation strength in the trajectory space.

Apart from these technical aspects of the SSA performance one has to consider the limitation of the method to linear feature extraction. Recall that SSA is called a "PCA in the time domain" which holds true for the technical implementation of the decomposition and also for the essential PCA outcome which is to achieve a dimensionality reduction. The main limitation of the presented SSA variant is its linear representation of the embedding space which is inherited from PCA. The question whether this is a suitable approach for dealing with real world data is not trivial. E.g., it is well known that PCA is a suboptimal solution for dimensionality reduction in nonlinear systems and could be replaced by nonlinear dimensionality reduction (Kramer, 1991). In accordance with this findings Hsieh and Wu (2001); Hsieh and Hamilton (2001) and Hsieh (2004) showed that the SSA results can be nonlinearly generalized at different levels, e.g., on the decomposition step, or by generalizing the RC's with artificial neural networks. On one hand, these features are principally challenging where the main advantage is that oscillatory modes of arbitrary shape can be represented by one single nonlinear component (Hsieh, 2004). On the other side such generalizations are fundamentally questionable; the critical point is that the mentioned neural network approaches rely

exclusively on previously linearly generated features, since the direct nonlinear feature extraction always leads to an parameter space which exceeded the number of observations. In this context new developments of data exploration (e.g. Coifman et al., 2005; Tenenbaum et al., 2000) could provide alternative solutions for a next generation of SSA.

3.5 Pattern extraction with missing data

In the context of eddy covariance measurements, missing data and rejected values, e.g., due to unfavorable conditions are unavoidable (Foken and Wichura, 1996). In terms of SSA applications this is especially problematic where more than 10% of data points where rejectedd and the method is operating at the very edge of a reasonable gap filling procedure (Kondrashov and Ghil, 2006).

Nevertheless, at first glance long continuous gaps could be effectively filled. Contrasting the SSA gap filled results with original fluxes indicates that the extracted low frequencies are not affected by the time series reconstruction based on a gappy time series (see Fig. 5). Indeed, the original paper on the SSA gapfilling suggests that the the method works optimal when only the on the leading modes are taken into account, while taking too much RC's into account increased the root mean square error of the procedure (Kondrashov and Ghil, 2006). This finding was confirmed by the present study and gives a repercussive justification for combining the gap filling strategy by Reichstein et al. (2005) for the high frequency data with the SSA application on the daily values.

This study did not carry out an in depth quality analysis, comparing the SSA based gap filling with established techniques as they are currently available (Moffat et al., 2007[2]); the presented application aims at giving a first impression how future gap filling strategies in the eddy covariance measurement setup could work. Specifically, it has to be sought to incorporate the potential of the information lying on the temporal correlation structure and the oscillatory components for improving the existing gap filling strategies which are relying on the "known" cross relationships of the variables. In fact, Kondrashov and Ghil (2006) introduced also the option for a multivariate SSA gap

filling. It has to be pointed out that the method is itself not in a fully maturated stage of development (cf. the current state of the discussion: Kondrashov and Ghil, 2007; Schneider, 2007). Despite of these details the SSA gapfilling is already a considerable progress for dealing with cases where, e.g., due to power breaks none of the target variables or standard meteorological observations are available. In these cases most gap filling methods fail, since they rely on a entirely sampled variable space (Falge et al., 2001; Papale and Valentini, 2003; Reichstein et al., 2005). The fundamental advantage in the SSA application is that the temporal correlation structure can be learned and projected to the data gaps, rather than introducing assumptions on cross relationships within the observation space.

3.6 Implications for future flux assessment and outlook

We showed that SSA provided a new way to partition the ecosystem flux variability into different time scales. There is considerable research interest in such data adaptive tools for assessing ecosystem-atmosphere carbon, water and energy fluxes. The application of advanced time series techniques could reveal further unexpected patterns, previously hidden in the raw data. There are many possible fields of application for SSA and related methods in addition to the presented "variance partitioning": for instance advanced flux partitioning methods which separate the contributions of *GPP* and R_{eco} to the net carbon flux. Comparisons between different flux partitioning methods showed that there are essential differences between the different approaches, but also that all known methods make comparable assumptions on underlying physiological kinetics (Stoy et al., 2006). The question is whether these models could be refined and validated on different time scales as we found them by SSA. What does it mean for example that a T record does not display the low frequency modes contained in the respective *NEE* data as it was found here? With this we aim at stimulating further discussions on how future flux partitioning algorithms could work taking the different behaviour of the variables on different time scales into account.

A main advantage is that the partly reconstructed variables can be further analysed in analogy to existing approaches which conventionally take the whole data series into

account. Figure 6 gives such an simple application example: Based on the annual-interannual components of *NEE*, *T*, and *LE* we estimated a mean seasonal course for each of them. This reference series was used to calculate and visualize the deviations of the respective RC's (Fig. 6). This enables us, e.g., to show how the summer drought which affected the site in 2003 is ongoing with a positive deviation of *NEE*; it turned out that the *NEE*-anomaly of the following year 2004 is equally pronounced. Moreover, the *T* record shows a smooth variation over the years indicating a systematic amplitude shift. A more complicated pattern is found in the behaviour of *LE*, which is apparently not trivially related to the other two variables. Without going into a detailed discussion, this example illustrates how powerful even simplistic approaches become when the time series are explicitly explored on the relevant temporal scales only. Extending the observation period in future investigations is expected to give major insights into the effects of time lagged ecophysiological responses to climate anomalies which in turn could improve our general understanding of ecosystem-atmosphere relationships.

4 Conclusions

Ecosystem-atmosphere interactions inferred from eddy covariance data are now comprising a time window which allows to investigate the flux behaviour beyond annual cycles. This study showed that applying advanced time series analysis methods allows to extract a wide range of significant modes ranging from the high frequency domain to long term components. A major innovation of the presented approach is to provide an integrated methodological framework comprising data analysis including signal to noise enhancement, and gap-filling and which in a next step could be expandable to a statistical time series forecast (Golyandina and Stepanov, 2005).

SSA proved to be able to separate the inherent temporal scales of a time series. Here, we showed that this "variance partitioning" could serve as general basis of further data adaptive or process oriented modelling tasks. Based on these methodological advances we were able to demonstrate that the eddy covariance observations are

dominated to a non negligible extent by interannual variability. Overall, the investigation showed that the relationships of water, carbon and energy fluxes are mostly nonlinear and vary fundamentally depending on the investigated temporal scale. For the first time we showed that hysteretic behaviour is an inherent property of ecosystem-interactions on an annual time scale.

Acknowledgements. This work is part of the integrated project "Carboeurope" (GOCE-CT2003-505572) of the European Union. M. D. Mahecha and M. Reichstein would like to thank the Max-Planck Society for supporting the "Biogeochemical Model-Data Integration Group" as Independent Junior Research Unit. This research was funded in part by the Marie Curie European Reintegration Grant "GLUES" (MC MERG-CT-2005-031077).

References

Allen, M. R. and Smith, L. A.: Monte Carlo SSA: Detecting irregular oscillations in the presence of coloured noise, Journal of Climate, 9, 3373–3404, 1996. 1408, 1411, 1412

Aubinet, M., Grelle, A., Ibrom, A., Rannik, Ü., Moncrieff, J., Foken, T., Kowalski, A. S., Martin, P. H., Berbigier, P., Bernhofer, C., Clement, R., Elbers, J., Granier, A., Grünwald, T., Morgenstern, K., Pilegaard, K., Rebmann, C., Snijders, W., Valentini, R., and Vesala, T.: Estimates of the annual net carbon and water exchange of forests: the EUROFLUX methodology, Adv. Ecol. Res., 30, 113–175, 2000. 1406, 1413

Baldocchi, D.: Assessing the eddy covariance technique for evaluating carbon exchange rates of ecosystems: past, present and future, Global Change Biol., 9, 479–492, 2003. 1406, 1407

Broomhead, D. S. and King, G. P.: Extracting qualitative dynamics from experimental data, Physica D, 20, 217–236, 1986. 1407

Ciais, P., Reichstein, M., Viovy, N., Granier, A., Ogée, J., Allard, V., Buchmann, N., Aubinet, M., Bernhofer, C., Carrara, A., Chevallier, F., Noblet, N. D., Friend, A., Friedlingstein, P., Grünwald, T., Heinesch, B., Keronen, P., Knohl, A., Krinner, G., Loustau, D., Manca, G., Matteucci, G., Miglietta, F., Ourcival, J. M., Pilegaard, K., Rambal, S., Seufert, G., Soussana, J. F., Sanz, M. J., Schulze, E. D., Vesala, T., and Valentini, R.: Europe-wide reduction in primary productivity caused by the heat and drought in 2003, Nature, 437, 529–533, 2005. 1418

Coifman, R. R., Lafon, S., Lee, A. B., Maggioni, M., Nadler, B., Warner, F., and Zucker, S. W.:

Geometric diffusions as a tool for harmonic analysis and structure definition of data: Diffusion maps, Proceedings of the National Academy of Sciences, 102, 7426–7431, 2005. 1421

Dunn, A. L., Bardford, C. C., Wofsy, S. C., Goulden, M. L., and Daube, B. C.: A long-term record of carbon exchange in a boreal black spruce forest: means, responses to interannual variability, and decadal trends, Global Change Biol., 577–590, doi:10.1111/j.1365-2486.2006.01221.x, 2007. 1407

Falge, E., Baldocchi, D., Olson, R. J., Anthoni, P., Aubinet, M., Bernhofer, C., Burba, G., Ceulemans, R., Clement, R., Dolman, H., Granier, A., Gross, P., Grünwald, T., Hollinger, D., Jensen, N.-O., Katul, G., Keronen, P., Kowalski, A. nad Ta Lai, C., Law, B. E., Meyers, T., Moncrieff, J., Moors, E., Munger, J. W., Pilegaard, K., Rannik, Ü., Rebmann, C., Suyker, A., Tenhunen, J., Tu, K., Verma, S., Vesala, T., Wilson, K., and S., W.: Gap filling strategies for longterm energy flux data sets, Agric. Forest Meteorol., 107, 71–77, 2001. 1422

Foken, T. and Wichura, B.: Tools for quality assessment of surface-based flux measurements, Agric. Forest Meteorol., 78, 83–105, 1996. 1421

Ghil, M. and Vautard, R.: Interdecadal oscillations and the warming trend in global temperature time series, Nature, 350, 324–327, 1991. 1407, 1415

Ghil, M., Allen, M. R., Dettinger, M. D., Ide, K., Kondrashov, D., Mann, M. E., Robertson, A. W., Saunders, A., Tian, Y., Varadi, F., and Yiou, P.: Advanced spectral methods for climatic time series, Rev. Geophys., 40, 1–25, 2002. 1407, 1411, 1420

Golyandina, N. and Stepanov, D.: SSA-based approaches to analysis and forecast of multidimensional time series, in: Proceedings of the 5th St.Petersburg Workshop on Simulation, pp. 293–298, St. Petersburg State University, St. Petersburg, 2005. 1423

Golyandina, N., Nekrutkin, V., and Zhigljavsky, A.: Analysis of Time Series Structure: SSA and related techniques, no. 90 in Monographs on Statistics and Applied Probability, Chapman & Hall/CRC, Boca Raton, 2001. 1408, 1409, 1411, 1419, 1420

Goulden, M. L., Munger, J. W., Fan, S. M., Daube, B. C., and Wofsy, S. C.: Exchange of Carbon Dioxide by a Deciduous Forest: Response to Interannual Climate Variability, Science, 271, 1576–1578, 1996. 1407

Granier, A., Reichstein, M., Brédaa, N., Janssens, I. A., Falge, E., Ciais, P., Grünwald, T., Aubinet, M., Berbigier, P., Bernhofer, C., Buchmann, N., Facini, O., Grassi, G., Heinesch, B., Ilvesniemi, H., Keronen, P., Knohl, A., Köstner, B., Lagergren, F., Lindroth, A., Longdoz, B., Loustau, D., Mateus, J., Montagnani, L., Nyst, C., Moorsu, E., Papale, D., Peiffer, M., Pilegaard, K., Pita, G., Pumpanen, J., Rambal, S., Rebmann, C., Rodrigues, A., Seufert, G.,

Tenhunen, J., Vesala, T., and Wang, Q.: Evidence for soil water control on carbon and water dynamics in European forests during the extremely dry year: 2003, Agric. Forest Meteorol., 143, 123–145, 2007. 1418

Grünwald, T. and Bernhofer, C.: A decade of carbon, water and energy flux measurement of an old spruce forest at the Anchor Station Tharandt, Tellus B, doi:10.111/j.1600-0889.2007.00259.x, 2007. 1414

Hsieh, W.: Nonlinear multivariate and time series analysis by neural network methods, Rev. Geophys., 42, 1–25, 2004. 1420

Hsieh, W. and Hamilton, K.: Nonlinear singular spectrum analysis of the tropical stratospheric wind, Q. J. R. Meteorol. Soc., 129, 2367–2382, 2001. 1420

Hsieh, W. and Wu, A.: Nonlinear multichannel singular spectrum analysis of the tropical Pacific climate variability using a neural network approach, J. Geophys. Res., 107(C7), 3076, doi:10.1029/2001JC000957, 2001. 1410, 1420

Katul, G., Lai, C.-T., Schäfer, K., Vidakovic, B., J., A., Ellsworth, D., and Oren, R.: Multiscape analysis of vegetation surface fluxes: from seconds to years, Adv. Water Resour., 24, 1119-1132, 2001. 1412

Kondrashov, D. and Ghil, M.: Spatio-temporal filling of missing data in geophysical data sets, Nonlin. Processes Geophys., 13, 151-159, 2006, http://www.nonlin-processes-geophys.net/13/151/2006/. 1408, 1412, 1421

Kondrashov, D. and Ghil, M.: Reply to T. Schneiders comment on “Spatio-temporal filling of missing points in geophysical data sets”, Nonlin. Processes Geophys., 14, 3–4, 2007, http://www.nonlin-processes-geophys.net/14/3/2007/. 1422

Kramer, M. A.: Nonlinear principal component analysis using autoassociative neural networks, AIChE Journal, 37, 233–243, 1991. 1420

Lange, H. and Bernhardt, K.: Long-term components and regional synchronization of river runoffs, in: Hydrology: Science and Practice for the 21st Century, edited by Butler, A., British Hydrological Society, London, 2004. 1407, 1420

Law, B. E., Falge, E., Gu, L., Baldocchi, D., Bakwin, P., Berbigier, P. Davis, K. J., Dolman, H., Falk, M., Fuentes, J., Goldstein, A. H., Granier, A., Grelle, A., Hollinger, D., Janssens, I., Jarvis, P., Jensen, N. O. Katul, G., Malhi, Y., Matteucci, G., Monson, R., Munger, J., Oechel, W., Olson, R., Pilegaard, K., Paw, U. K. T., Thorgeirsson, H., Valentini, R., Verma, S., Vesala, T., Wilson, K., and Wofsy, S.: Carbon dioxide and water vapor exchange of terrestrial vegetation in response to environment, Agric. Forest Meteorol., 113, 97–120, 2002. 1407

Nakai, Y., Kitamura, K., and Abe, S.: Year-long carbon dioxide exchange above a broadleaf deciduous forest in Sapporo, Northern Japan, Tellus B, 55, 305–312, 2003. 1418

Paluš, M. and Novotná, D.: Enhanced Monte Carlo SSA and the case of climate oscillations, Phys. Lett. A, 248, 191–202, 1998. 1411

Paluš, M. and Novotná, D.: Quasi-biennial oscillations extracted from the monthly NAO index and temperature records are phase-synchronized, Nonlin. Processes Geophys., 13, 287–296, 2006, http://www.nonlin-processes-geophys.net/13/287/2006/. 1407, 1415

Papale, D. and Valentini, R.: A new assessment of European forests carbon exchanges by eddy fluxes and artificial neural network spatialization, Global Change Biol., 9, 525–535, 2003. 1422

Papale, D., Reichstein, M., Aubinet, M., Canfora, E., Bernhofer, C., Kutsch, W., Longdoz, B., Rambal, S., Valentini, R., Vesala, T., and Yakir, D.: Towards a standardized processing of Net Ecosystem Exchange measured with eddy covariance technique: algorithms and uncertainty estimation, Biogeosciences, 3, 571–583, 2006, http://www.biogeosciences.net/3/571/2006/. 1413

Peters, O., Hertlein, C., and Christensen, K.: A Complexity View of Rainfall, Physical Review Letters, 88, 018 701–1–018 701–4, 2002. 1415

Plaut, G. and Vautard, R.: Spells of low-frequency oscillations and weather regimes in the Northern Hemisphere, J. Atmos. Sci., 51, 210–236, 1994. 1407

Plaut, G. and Vautard, R.: Interannual and interdecadal variability in 335 years of Central England temperatures, Science, 268, 710–713, 1995. 1407

Reichstein, M., Falge, E., Baldocchi, D., Papale, D., Valentini, R., Aubinet, M., Berbigier, P., Bernhofer, C., Buchmann, N., Gilmanov, T., Granier, A., Grünwald, T., Havrnkov, K., Janous, D., Knohl, A., Laurila, T., Lohila, A., Loustau, D., Matteucci, G., Meyers, T., Miglietta, F., Ourcival, J.-M., Rambal, S., Rotenberg, E., Sanz, M., Seufert, G., Vaccari, F., Vesala, T., and Yakir, D.: On the separation of net ecosystem exchange into assimilation and ecosystem respiration: review and improved algorithm, Global Change Biol., 11, 1–16, 2005. 1414, 1421, 1422

Reichstein, M., Ciais, P., Papale, D., Valentini, R., Running, S., Viovy, N., Cramer, W., Granier, A., Ogé, J., Allard, V., Aubinet, M., Bernhofer, C., Buchmann, N., Carrara, A., Grünwald, T., Heinesch, B., Keronen, P., Knohl, A., Loustau, D., Manca, G., Matteucci, G., Miglietta, F., Ourcival, J. M., Pilegaard, K., Rambal, S., Schaphoff, S., Seufert, G., Soussana, J.-F., Sanz, M.-J., Schulze, E. D., Vesala, T., and Heimann, M.: A combined eddy covariance, remote

sensing and modeling view on the 2003 European summer heatwave, Global Change Biol., 13, 634651, 2007. 1418

Saigusa, N., Yamamoto, S., Murayama, S., and Kondo, H.: Inter-annual variability of carbon budget components in an AsiaFlux forest site estimated by long-term flux measurements, Agric. Forest Meteorol., 134, 4–16, 2005. 1406

Schneider, T.: Comment on “Spatio-temporal filling of missing points in geophysical data sets” by D. Kondrashov and M. Ghil, Nonlin. Processes Geophys., 13, 151-159, 2006, Nonlin. Processes Geophys., 14, 1–2, 2007, http://www.nonlin-processes-geophys.net/14/1/2007/. 1422

Shun, T. and Duffy, C.: Low-frequency oscillations in precipitation, temperature, and runoff on a west facing mountain front: A hydrogeologic interpretation, Water Resour. Res., 35, 191–201, 1999. 1407, 1411, 1412, 1415

Stoy, P. C., Katul, G. G., Siqueira, M. B. S., Juang, J.-Y., Novick, K. A., Joshua, M., Uebelherr, and Oren, R.: An evaluation of models for partitioning eddy covariance-measured net ecosystem exchange into photosynthesis and respiration, Agric. Forest Meteorol., 141, 2–18, 2006. 1422

Tenenbaum, J. B., de Silva, V., and Langford, J. C.: A global geometric framework for nonlinear dimensionality reduction, Science, 290, 2319–2323, 2000. 1421

Tessier, Y., Lovejoy, S., Hubert, P., Schertzer, D., and Pecknold, S.: Multifractal analysis and modeling of rainfall and river flows and scaling, causal transfer functions, J. Geophys. Res., 101(D21), 26 427–26 440, 1996. 1415

Vautard, R. and Ghil, M.: Singular spectrum analysis in nonlinear dynamics, with applications to paleoclimatic time series, Physica D, 35, 395–424, 1989. 1409

von Storch, H. and Zwiers, F.: Statistical Analysis in Climate Research, Cambridge University Press, Cambridge, 1999. 1407

Wilson, K. and Baldocchi, D.: Seasonal and interannual variability of energy fluxes temperate deciduous forest in North America, Agric. Forest Meteorol., 100, 1–18, 2000. 1407

Table 1. Significant periods identified in the flux time series. The periods are given in years (rounded values). Modes at the edge of the maximal observed frequency domain (here, 3.4 years) could be either "real" trends or edge cycles. The values of the variables at the respective period indicate the amount of explained variance in percentages. Note that each value is the sum of explained variance for all significant components of similar period, e.g., the annual components are always set up by two EOF's.

Period p (years)	*NEE*	*GPP*	R_{eco}	*T*	R_g	*VPD*	*P*	*LE*	*H*	*u*
≥3.4	0.8	0.5	3.7	–	–	–	–	2.2	1.4	–
2.4	–	–	2.4	–	–	0.6	–	–	–	–
2.3	–	0.5	–	–	–	–	–	1.1	–	–
1.8	–	–	0.6	–	–	–	–	–	–	1.4
1.7	–	0.3	–	–	–	–	–	–	0.6	–
1.4	–	0.1	–	–	0.2	0.5	0.7	2.6	–	–
1	55.6	80.7	74.5	69.2	60.6	38.9	–	60.4	37.5	8.8
0.8	–	0.3	0.4	–	–	–	–	0.5	0.9	–
0.7	–	0.1	–	–	–	1.1	–	–	–	0.7
0.6	0.2	0.9	1.5	–	0.5	–	–	2.4	–	–
0.5	0.7	0.4	1.6	–	0.2	1.7	–	0.7	0.7	–
0.4	0.6	0.2	–	–	–	–	–	0.9	–	0.9
0.3	1.4	0.6	–	–	0.5	1.3	–	1.5	1.1	1.2
0.2	0.8	0.3	–	–	0.7	1.6	–	0.8	0.5	3.1
0.1	1.7	1.8	–	–	1.4	–	1.8	4.2	5.2	8.1
<0.1	1.1	0.5	–	–	0.8	–	–	1.5	1.4	–
red noise	38.1	12.9	15.3	30.8	35.1	54.3	97.5	21.3	50.6	75.0

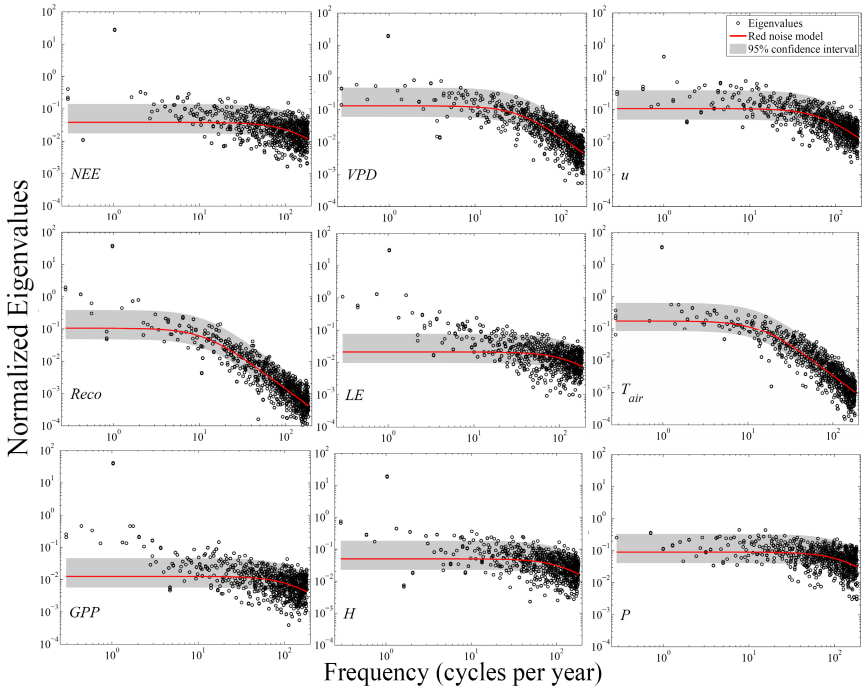

Fig. 1. The eigenspectra of the observed time series for *NEE*, R_{eco}, *GPP*, *VPD*, *LE*, *H*, *u*, *T*, and *P*. The dots represent the dominant frequencies of the time series at the respective normalized eigenvalue. The latter is equivalent to the amount of allocated variance. The red lines show the fitted red noise model. The gray areas are the corresponding 95% significance intervals.

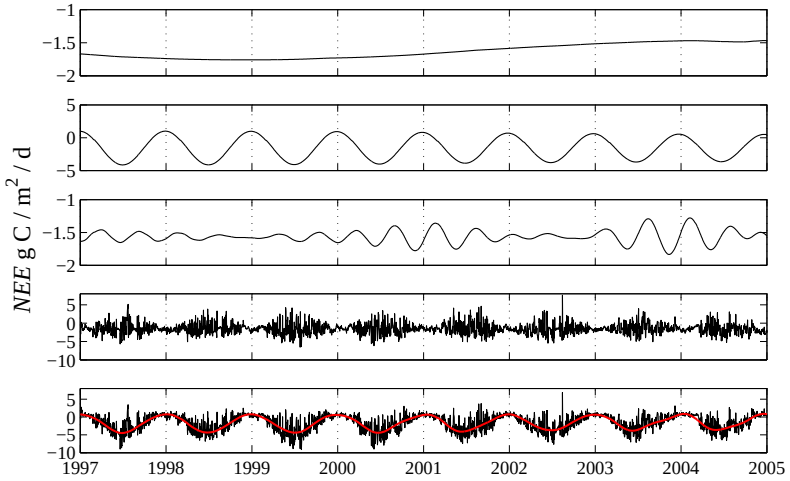

Fig. 2. The partly reconstructed NEE flux time series. From top to bottom: the interannual variability; the annual cycle; the semiannual oscillation; the time series reconstruction from the components which were not distinguishable from red noise; the original signal (black line) and the reconstructed signal based on the above shown significant modes (red line).

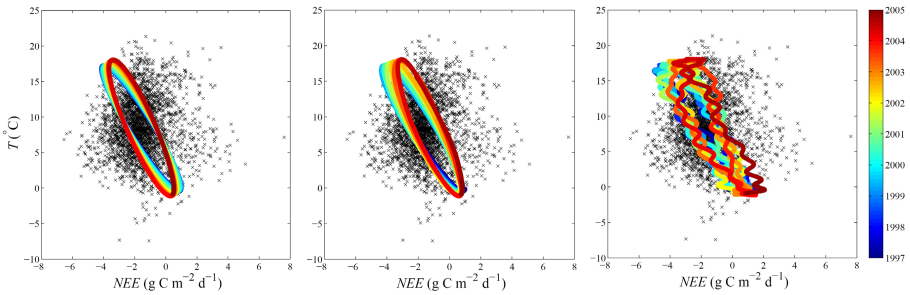

Fig. 3. The cross relationship of the partly reconstructed *NEE* and *T* time series. From left to right: The first panel shows the pure annual components of both variables where the colour code permits tracing the temporal evolution. The black crosses show the respective red noise components. The centre panel time series reconstruction is based on the annual and interannual components. The right panel shows a reconstruction, where also the significant intraannual components were considered.

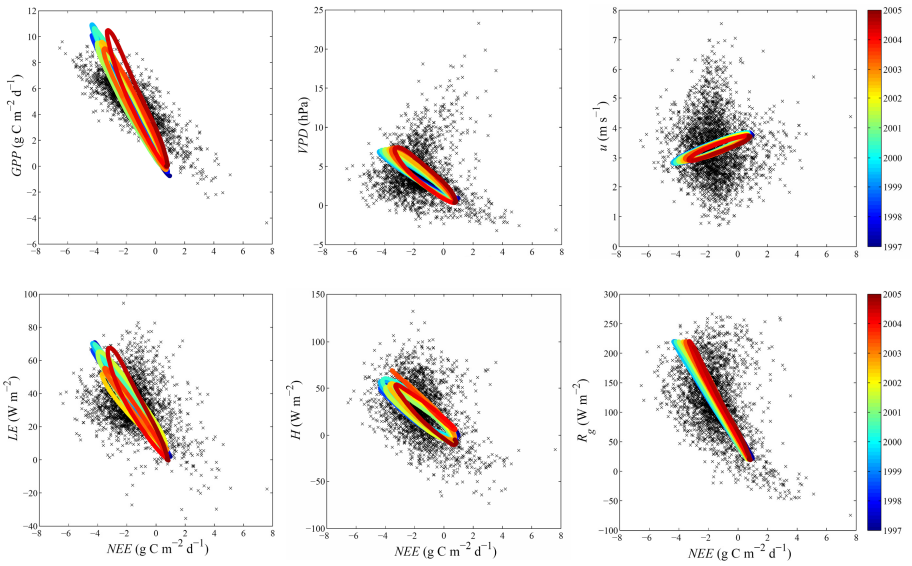

Fig. 4. The cross relationships of the major variables with *NEE*. Black crosses show the respective red noise components. The colour coded reconstructed components comprise the annual and interannual components of the respective variables, where the colour code permits tracing the temporal evolution.

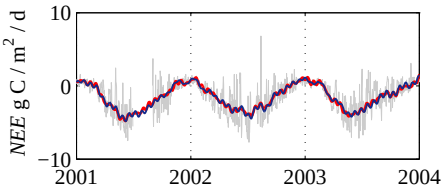

Fig. 5. The reconstruction of the *NEE* time series based on all significant components (red line). The reconstruction is repeated after an artificially gap of three month was generated (blue line).

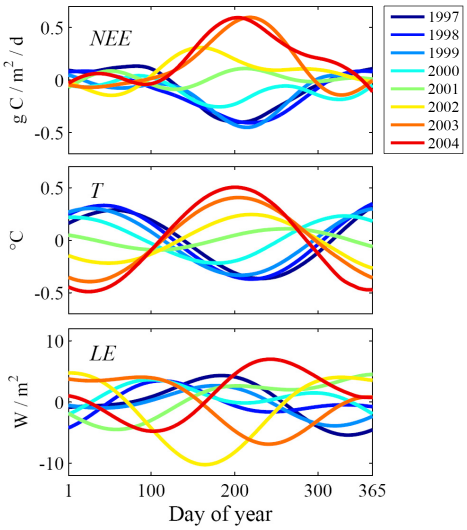

Fig. 6. The deviations of the estimated mean reference component of *NEE*, *T* and *LE*, based on the joint reconstruction of the annual and interannual components.